Mathematical Biosciences and Engineering

MBE, 20(9): 15708–15736.
DOI: 10.3934/mbe.2023700
Received: 21 April 2023
Revised: 28 June 2023
Accepted: 07 July 2023
Published: 28 July 2023

http://www.aimspress.com/journal/MBE

Research article

Research on charging behavior of electric vehicles based on multiple objectives

Tien-Wen Sung, Wei Li*, Qiaoxin Liang*, Chuanbo Hong and Qingjun Fang

Fujian Provincial Key Laboratory of Big Data Mining and Applications, College of Computer Science and Mathematics, Fujian University of Technology, Fuzhou, China

* **Correspondence:** Email: liwei19980623@gmail.com, 773590899@qq.com.

Abstract: This paper proposes a multi-objective queuing charging strategy for electric vehicles (EVs) based on metrics of public interest. It combines common charging modes, such as random charging mode, tariff-guided mode and stop-and-charge mode. It introduces the problem of queuing charging for EVs by considering the realistic imbalances of vehicle-pile ratios in these common modes. A travel model and a charging model were developed in this study. Experiments prove that the proposed strategy has the highest comprehensive evaluation index, achieves the aim of low charging cost and high travel rate and considers the queuing problem, which is unavoidable in reality. It improves the convenience of life and reduces the charging cost. The proposed strategy smoothens the EV charging load curve, largely reducing the burden of charging load fluctuations on the grid and achieving a win-win situation for both supply and demand.

Keywords: electric vehicle charging; queuing charging; multi-objective optimization; vehicle-pile ratios; grid load

1. Introduction

With the gradual deterioration of air quality and the environment and the energy crisis caused by fuel cars worldwide, renewable energy vehicles, i.e., electric vehicles (EVs), have been strongly promoted by governments of various countries. EVs have been developing rapidly due to the gradual improvement of the system and the construction of related infrastructure. However, this entails a new test for vehicle charging equipment and its power supply system [1]. Constructing charging facilities will also put forward higher requirements, where the scale and use area of charging facilities must be larger and wider.

As the energy demand for EVs continues to increase, the uncertainty of grid regulation becomes increasingly serious, bringing huge deployment pressure on the grid. The load demand of an average electric vehicle is usually equivalent to the electricity consumption of an average household when connected to the grid. In addition, EVs have several impacts on the distributed grid. Their influencing factors can generally be divided into the following: penetration rate, battery characteristics, driving mode and charging schedule [2–5]. The impact of EV access on the grid is shown in Figure 1.

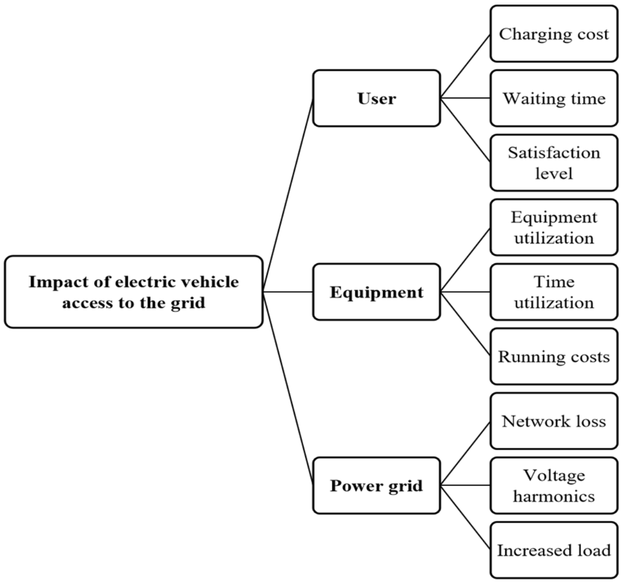

Figure 1. Impact of electric vehicle access to the grid.

The two factors that generally determine the charging scheme of EVs are the charging strategy and the charging situation [6]. Since the daily energy consumption of an EV is smaller than the rated power of the battery itself, the need for daily charging is eliminated, and the EV only requires recharging when the battery state of charge (SOC) is less than the set threshold. Generally, the charging modes of EVs can be divided into the following [7]: 1. Tariff-guided charging mode (i.e., users charge their EVs during non-peak hours to avoid high charges); 2. Simple direct charging mode (i.e., users charge by “plug-and-charge,” where there is no need to plan, and they can charge at any time, which is more arbitrary); 3. Smart charging mode, in which EV users can sell excess battery energy to the grid during peak hours as an energy resource for auxiliary services, which not only contributes to the operational stability of the grid [8] but also offsets some of the charging costs.

For general research, most EVs’ charging modes are based on tariff-guided charging and discharging research. These modes can effectively avoid charging Evs during the peak hours of electricity consumption, which can reduce the pressure on the power grid and reduce the charging costs of users. However, only using the electricity tariff-guided charging and discharging strategy causes a new peak at night, when the electricity price is lowest, which seriously affects the stable operation of the power grid. In addition, it does not take into account some emergency situations, such as users urgently needing a car and not having the time to wait. Thus, only considering the tariff factor is far from enough. To further increase user support for the orderly charging and discharging strategy, one should consider not only the economy, stability and safety of the grid but also the actual demand, economic efficiency and cost performance for the user [9–12].

Large-scale electric vehicle charging behavior is one of the popular topics currently receiving public attention and has a significant impact on the daily lives of contemporary residents [13]. However, most of the current research findings on large-scale EV charging behavior do not take into account the realistic condition of the limitation of the number of charging piles. Therefore, this paper uses this as the subject with the following main contributions:

Given the current charging pile coverage degree, a multi-objective EV queuing charging strategy is proposed, in which several EVs must be charged simultaneously in a limited number of charging piles. The strategy divides the battery capacity of EVs into large-capacity and small-capacity batteries according to the actual situation. Since batteries of different capacities have different demands for daily travel, the charging priority of EVs is set accordingly, and EVs are queued for charging according to the charging priority.

The proposed strategy is divided into five modes: random charging queuing mode, tariff-guided queuing mode, stop-and-charge queuing mode, emergency charging mode and combined charging queuing mode.

In order to achieve the performance of the strategy, an EV travel model and a charging model are established. An orderly queuing strategy is also used to alleviate the phenomenon, minimize the charging cost of users and reduce the valley-peak difference while taking into account the actual situation of an unbalanced vehicle-pile ratio, thereby avoiding imposing a large load on the grid.

The rest of this paper is organized as follows. Section 2 presents the related work. Section 3 establishes the travel model and charging model of EVs and proposes a multi-objective EV queuing charging strategy based on multiple objectives. Section 4 introduces the Monte Carlo (MC) simulation and queuing charging processes and establishes the objective function to select the intelligent optimization algorithm. Section 5 provides a comprehensive analysis of the multi-objective EV charging behavior using the intelligent optimization algorithm and compares the performances of the models in all aspects. Section 6 draws conclusions and discusses future work.

2. Related works

Xu et al. [14] proposed a multi-energy management strategy that calculates several EV priorities to form an EV charging and discharging priority table through scheduling, aiming to reduce power fluctuations in the grid and meet the daily usage requirements of EV users. Xiao et al. [15] proposed to minimize the charging cost of EV charging stations and the operating cost of microgrids by developing a real-time tariff strategy and an orderly charging and discharging strategy. He et al. [16] performed a simulation of users' driving behavior and considered the behavior of random charging of EVs. A two-level charging control strategy was proposed for the charging problem of EVs, and its feasibility was verified by simulating each of the four scenarios. Sachan and Adnan [17] evaluated the impact of different EV charging methods on the distribution grid to achieve the optimal amount of EV charging without changing the grid or enhancing the grid infrastructure. While they also optimized the losses in the grid and reduced the charging costs, the article only considered the charging of EVs for home use. Yan et al. [18] proposed formulating the EV charging problem as a Markov game with an unknown transfer function and proposed a collaborative charging control strategy based on deep reinforcement learning (DRL) of multiple intelligences. Ping et al. [19] proposed a two-stage EV charging coordination mechanism that frees the distribution system operator (DSO) from the additional burden of EV charging coordination.

In terms of the relationship between the grid and EVs, it is crucial to discuss Vehicles-To-Grid (V2G)-a technology proposed in 1995. In V2G, EVs connected to the supply side act not only as a load but also as a distributed power source, allowing them to share the load pressure while consuming excess power from the grid. It is undoubtedly an indispensable technology that relieves the pressure on the grid. Iqbal et al. [20] proposed that to ensure that the electric vehicle charging state is maintained at the desired charging state, the power supply must be rectified in real time using V2G. A V2G control strategy for microgrid primary frequency control was developed to arrange supervision for each EV. This strategy allows for reasonable coordination between the three parties-EV operators, aggregators and charging stations. Optimization problems exist in various industries, such as engineering optimization, neural network optimization, and intelligent computing, all of which require efficient and accurate optimization algorithms [21]. Akram et al. [22] used particle swarm optimization to enable EV V2G to run until the time period when electricity prices were higher, minimizing the cost of electricity to the user. Chen et al. [23] studied a method to evaluate the impact of EV participation in charging and discharging on the voltage quality of the distribution network. First, the charging and discharging model was established by considering the charge state of EVs and other factors. Then, a probabilistic current calculation based on Latin hypercube sampling was used to obtain the probability distribution of the voltage magnitudes of charging and discharging loads in the distribution network. Finally, evaluation indexes were established to quantify the voltage quality of the distribution network. An ordered charging and discharging strategy based on V2G was proposed in [24]. In particular, a charging and discharging load model was proposed which considered and maximized the benefits of both the supply and demand sides. Several commonly used models were compared by considering the aspects of grid capacity, start time of charging and the presence of randomness in the duration. The valley-peak variance of the grid load was minimized, and the cost of electricity for customers was reduced. DRL is a combination of reinforcement learning (decision-making capability) and deep learning (perceptual function) that can solve the challenging problem of sequential decision-making. DRL can be used in various applications, such as power system operation control, autonomous Internet of Things (AIoT) [25] and electric vehicle charging scheduling. Lee et al. [26] proposed a model-free DRL based algorithm for optimal path and charging station selection (RCS) to address the uncertainty of traffic conditions and dynamic arrival charging requests.

3. System model establishment

The demand for electric vehicle charging remains high in proportion to the total electricity consumption of society as a whole, which is a new test for charging facilities and the grid system. Due to the limited charging conditions and national grid constraints, it is crucial to predict the driving and charging behaviors of EVs. In this section, the MC method is proposed to model the travel and charging of EVs.

3.1. EV travel model

While there is a certain regularity in each EV user's daily travel habits and car use behavior, each user's habits are still different [27]. In using the MC method for modeling, users' travel habits must be considered a key part of the modeling process and fully understood. These travel habits include the frequency of daily trips and the mileage, time distribution and departure time of each trip. The distribution functions of these travel habits can be derived based on the results of the survey in the relevant sectors [27–29].

MC is a mathematical method based on probability statistics and mathematical analysis. First, the probability of the entire event occurring is constructed or described. Second, a random sample is used to sample the current probability model. Finally, unbiased estimators are constructed. This method not only responds to the process that coincides with objective laws but also yields more realistic results used frequently in many settings.

In this paper, we apply maximum likelihood estimation (MLE) to estimate the parameters, generally based on the known model. However, some of the parameters inside the model are still unknown, in which case the MLE can be used to find the parameter with the highest probability in the sample.

The distance per trip for EV users follows the Birnbaum-Saunders (BS) distribution. The distribution function $F(x)$ and the probability density function $f(x)$ are presented in Eqs (1) and (2), respectively:

$$F(x) = \Phi\left[\frac{1}{\omega}\left(\sqrt{\frac{x}{\beta}} - \sqrt{\frac{\beta}{x}}\right)\right] \tag{1}$$

$$f(x) = \frac{1}{2\omega x}\left(\sqrt{\frac{x}{\beta}} + \sqrt{\frac{\beta}{x}}\right) \cdot \varphi\left[\frac{1}{\omega}\left(\sqrt{\frac{x}{\beta}} - \sqrt{\frac{\beta}{x}}\right)\right], \quad x > 0 \tag{2}$$

where ω is the shape parameter, $\omega > 0$, and β is the scale parameter, $\beta > 0$. $\varphi(x) = 1/\sqrt{2\pi} * e^{-\frac{x^2}{2}}$ and $\Phi(x) = \int_{-\infty}^{x} \varphi(y)\, dy$ are the density and distribution functions of $N = (0,1)$, respectively. The MLE provides the following values: $\beta = 10.57, \omega = 0.97$, variance of 15.09 and mean of 15.52. The probability density distribution curve of the actual EV user data with the BS-fitted curve distribution is shown in Figure 2.

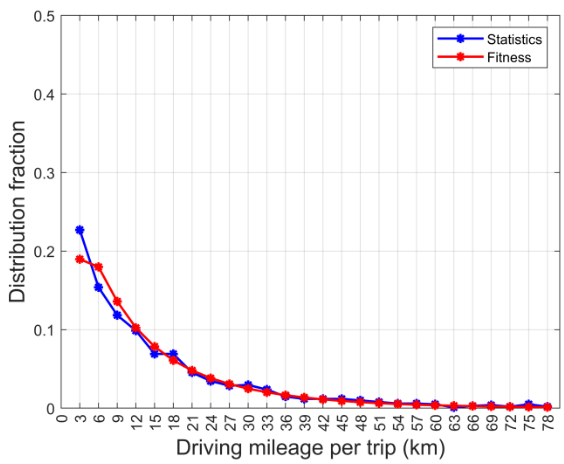

Figure 2. Distribution of distance per trip.

The daily trip frequency F_d following the Γ distribution and the probability density function $f(x|\alpha,\gamma)$ are shown in Eqs (3) and (4), respectively. $\Gamma(\alpha)$ is the gamma function, where α is the shape parameter, and γ is the scale parameter. The MLE provides the following values: $\alpha = 3.71$, $\gamma = 0.64$, variance of 1.24 and mean of 2.39. The comparison of the actual EV user data with the fitted curve of trip frequency is shown in Figure 3.

$$\Gamma(\alpha) = \int_0^{\infty} t^{\alpha-1} e^{-t}\, dt \tag{3}$$

$$f(x|\alpha,\gamma) = \frac{1}{\gamma^{\alpha}\Gamma(\alpha)} x^{\alpha-1} e^{-\frac{x}{\gamma}} \tag{4}$$

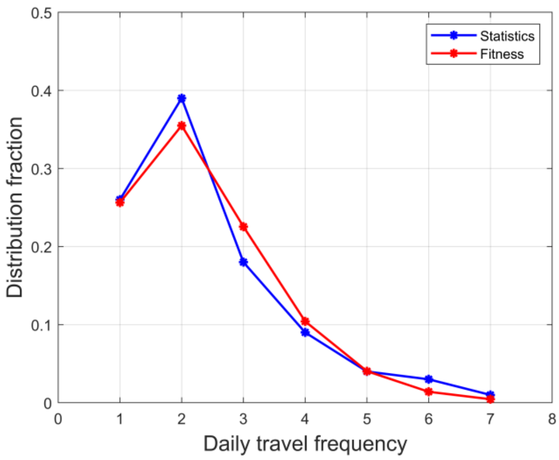

Figure 3. Distribution of daily trip frequency.

The duration of each trip T_d follows the same Γ distribution, according to Eqs (3) and (4). The parameters are obtained by MLE: $\alpha = 1.87$, $\gamma = 18.35$, with a variance of 25.12 and a mean of 34.4. A comparison of the fitted curve with a gamma distribution and the actual data curve is shown in Figure 4.

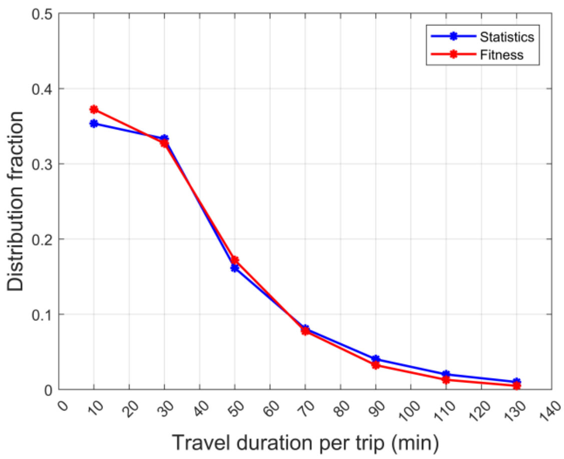

Figure 4. Distribution of duration per trip.

The departure time of each trip differs according to the function fitted to two different time periods. If the trip departure time is in the morning, it follows the location-scale distribution function. The probability density function of T_d^{am} is shown in Eq (5):

$$f_{T_d^{am}}(x|\delta,\varepsilon,\theta) = \frac{\Gamma\left(\frac{\theta+1}{2}\right)}{\varepsilon\cdot\sqrt{\pi\theta}\cdot\Gamma\left(\frac{\theta}{2}\right)}\cdot\left[\frac{\theta+\left(\frac{x-\delta}{\varepsilon}\right)^2}{\theta}\right]^{-\frac{\theta+1}{2}} \tag{5}$$

where $\Gamma(\cdot)$ denotes the gamma function, θ is the shape parameter, ε is the scale parameter, and δ is the position parameter. The above three parameters can be estimated by MLE with the following values: θ = 2.16, ε = 1.08, δ = 8.36 and a variance of 3.98.

If the travel departure time is afternoon T_d^{pm}, the probability density function will follow the normal distribution law, as shown in Eq (6).

$$f_{T_d^{pm}}(x|\delta,\varepsilon) = \frac{1}{\sqrt{2\pi}\varepsilon}\cdot e^{-\frac{(x-\delta)^2}{(2\varepsilon)^2}} \tag{6}$$

The parameters, δ = 18.2 and ε = 2.84, were obtained by maximum likelihood estimation. The fitted and actual data curves of the departure time probability density distribution for each electric vehicle trip are shown in Figure 5.

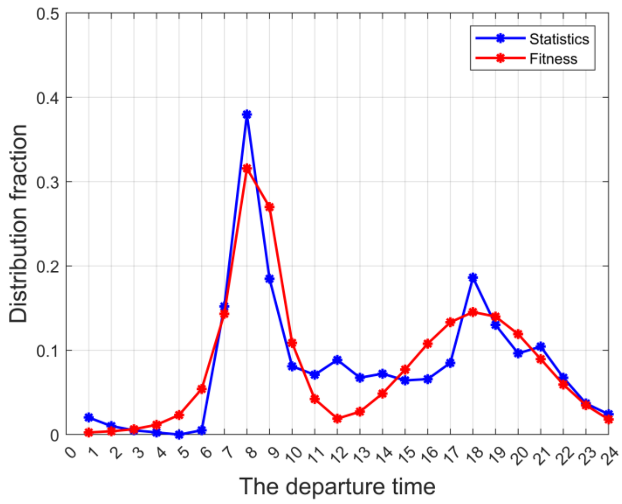

Figure 5. Distribution of departure time per trip.

SOC is a technical parameter used to represent the battery's charge state. The battery energy distribution can be seen from its size, which can also be used to determine the battery's performance. The definition of SOC can be expressed in Eq (7):

$$SOC = \frac{C_{curr}}{C_r} \tag{7}$$

where C_r represents the rated capacity size of the EV battery while C_{curr} represents the current capacity size of the EV battery.

3.2. Multi-objective EV charging model

The charging strategy and the charging situation are the two factors that determine the charging scheme. Further, the charging strategy must first be addressed in building a charging model for EVs. EV users choose different charging strategies (i.e., setting a specific charging target or choosing an optimal charging period) [30]. For example, an EV user chooses the lowest tariff moment for charging according to the different tariffs throughout the day to reduce the cost. This strategy is called a tariff-guided charging strategy. The three commonly used charging strategies are described in detail, as shown in Table 1.

Table 1. Description of basic charging strategy.

Strategy	Strategy Description
Random charging	EVs are charged at random moments of idleness.
Tariff-guided charging	EVs are charged at the time of day when electricity prices are lowest, reducing the cost of charging for EV users.
Stop-and-charge charging	If the parking time exceeds the charging time, then the EV is charged as soon as it arrives to keep the power in ideal condition and increase the success of the trip.

Several EVs simultaneously connected to the grid can cause a considerable disturbance–in serious cases, grid collapse. The results of the Beijing traffic survey [31] show that for private cars, the peak travel times are concentrated between 6:00 and 9:00 and between 16:00 and 19:00; for many EV users, the idle hours are mainly between 9:00 and 14:00 and between 20:00 and 23:00. EVs with random charging strategy and stop-and-charge charging strategy focus on charging in these two time periods, respectively. The charging load of EVs reaches two peaks, which are often peak periods of electricity consumption, as shown in Figure 6. In this case, the power grid will bear a double load of household electricity and EV charging simultaneously, causing serious power supply tension.

On the other hand, a tariff-guided charging strategy essentially means that EVs are charged when electricity prices are lowest, often between 23:00 and 4:00. Although EVs, under the guidance of a tariff-guided charging strategy, can avoid charging during peak hours, they can still generate a charging peak in a relatively short period of time from 23:00 to 2:00. Therefore, only using the tariff-guided charging strategy can effectively reduce the charging cost. However, there will still be a concentrated charging period at night, suddenly increasing the peak power consumption and seriously affecting the stability of the grid operation.

From a combined perspective, none of the three charging strategies provide satisfactory performance under single-factor considerations. For example, while the stop-and-charge strategy can ensure successful trips, increasing the success rate, it also generates higher bills and increases the burden of grid power supply; in addition, charging too frequently can harm battery life. If the charging strategy of tariff-guided is solely adopted, the charging cost of users can be reduced. However, in addition to causing load peaks in a short period of time, the required power cannot be guaranteed if urgent travel is required, which reduces the success rate of travel.

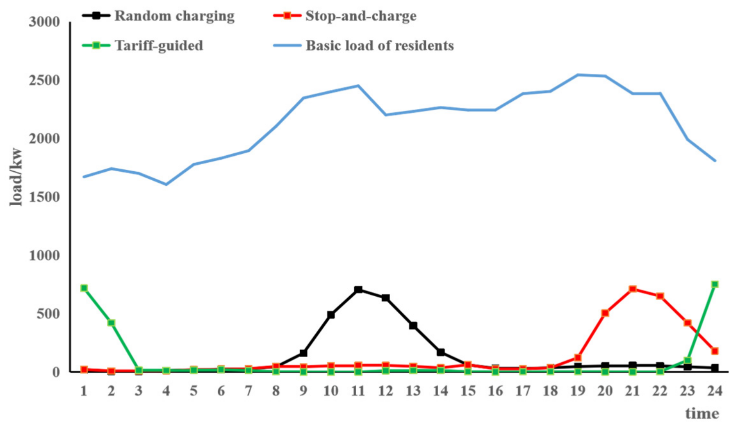

Figure 6. Hourly charging load under three different strategies and basic load of residents.

Further, the three charging strategies mentioned above do not consider the need for queuing for charging. With the increasing number of EVs, the total vehicle-pile ratio of new EVs in China has dropped to 3.1:1, and the public vehicle-pile ratio is only 6.5:1, according to the data published by China Charging Alliance, as shown in Figure 7, which means that the number of charging piles will not be able to meet the demand of new EV owners during the peak period of EV charging. In addition, the utilization rate of public charging piles in different urban areas is polarized, resulting in insufficient charging piles in some areas while many idle charging piles exist in others. The effective utilization rate of charging piles is far lower than the number of charging piles [32–33]. Therefore, a new strategy must be proposed to solve the problem of the mismatch between the cars and the piles.

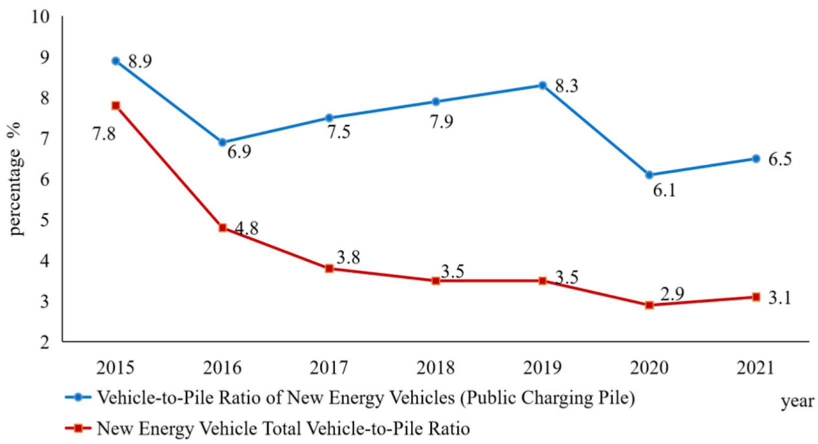

Figure 7. Vehicle-to-pile ratio of new energy vehicles in China.

Based on the problems presented above, the three charging strategies are added to optimize the EV queuing charging situation. A multi-objective EV queuing charging strategy that integrates travel success rate, charging cost-saving rate and grid load is also proposed, and a charging priority parameter is established to regulate the charging vehicles reasonably. The strategy combines several charging strategies commonly used in daily life, allowing users to independently choose charging targets according to their needs and EVs to choose the best charging time period in a day. It can achieve the purpose of peak-shaving and valley-filling, reducing the pressure on the grid while minimizing the charging cost for users. The combined charging strategy model is shown in Eq (8) to Eq (18). Several hypotheses are proposed for the model in this paper, as follows:

a) The batteries used in EVs are always kept at constant power from the beginning to the end of charging.
b) During the charging process, the relevant parameters of the charging piles used for EVs are the same, and no special distinction is made.
c) Throughout the study process, users charge according to their usual electricity habits.
d) In order to ensure that the original travel plan can be executed smoothly and reduce the damage to the battery, it is assumed that the battery pack will be charged up to 90% each time.
e) Dividing each day (i.e., 24 hours) equally into h period intervals, a sampling period is set to $1440/h$ minutes.

$$P_T = [S_1 + S_2 + S_3] * S_4 + S_5 + U(x) \tag{8}$$

$$P_C = [S_1 + S_2 + S_3 + F(s)] * S_4 + S_5 \tag{9}$$

$$S_1 = R * \varphi_1 \tag{10}$$

$$S_2 = (1.5 - \frac{\bar{C}_{\Delta T}}{\bar{C}_D}) * \varphi_2 \tag{11}$$

$$S_3 = (1.5 - \frac{T_{Charge}}{T_{Parking}}) * \varphi_3 \tag{12}$$

$$S_4 = (1 - \varphi_4) \tag{13}$$

$$S_5 = \varphi_4 * (+\infty) \tag{14}$$

$$U(x) = \begin{cases} 0, & other \\ +\infty, & 0 < SOC_{curr} < SOC_{min} \end{cases} \tag{15}$$

where P_T represents the priority of the EV in the current time period among h time periods per day. The EV starts charging when $P_T > 0.5$. The most suitable charging time period of the day with a comprehensive index can be calculated by P_T. P_C indicates the current queuing priority of EVs for charging, and the EVs that need to be charged in the current period are queued for charging according to the size of this priority. φ_i is the weighting factor, and R is the random priority factor that follows a uniform distribution, $R \in [0,1]$, such that the random charging behavior is simulated. T_{Charge} is the time used to fully charge the EV, and $T_{Parking}$ is the EV's parking time.

$$\varphi_4 \begin{cases} 0, & Normal\ mode \\ 1, & Emergency\ mode \end{cases} \tag{16}$$

$$\sum_{i=1}^{3} \varphi_i = 1 \tag{17}$$

$$(s)\begin{cases} +\infty, & 0 < SOC_{curr} < SOC_{bmin}\ or \\ & 0 < SOC_{curr} < SOC_{smin} \\ 0, & SOC_{bmin} < SOC_{curr} < 3SOC_{bmin}\ or \\ & SOC_{smin} < SOC_{curr} < 3SOC_{smin} \\ -0.2 * SOC_{curr}, & 3SOC_{bmin} < SOC_{curr} < 1\ or \\ & 3SOC_{smin} < SOC_{curr} < 1 \end{cases} \tag{18}$$

SOC_{curr} denotes the current SOC of EVs, SOC_{min} denotes the minimum SOC of high-capacity and small-capacity batteries, SOC_{bmin} denotes the minimum SOC of high-capacity batteries, and SOC_{smin} denotes the minimum SOC of small-capacity batteries. $F(s)$ indicates that if the current SOC of the EV is less than the minimum SOC, the EV is charged immediately. To ensure the reliability of the travel plan, SOC_{bmin} is set to 0.2, and SOC_{smin} is set to 0.25. When SOC_{curr} is greater than the set value, $F(s)$ is considered a negative function, which reduces the priority of charging. The above parameter φ_4 represents a switch. When φ_4 is 0, it means that the EV is in regular charging mode, and the emergency mode does not work. On the other hand, when φ_4 is 1 and S_4 is 0, it enters the emergency charging mode and charges the EV immediately. Those who choose the emergency charging mode will be charged with an additional charge.

$\bar{C}_{\Delta T}$ denotes the average charging cost of an EV over a period of time, and $\bar{C}_D$ denotes the average charging cost of an EV in a day. $\bar{C}_{\Delta T}$ is calculated using Eq (19) as follows:

$$\bar{C}_{\Delta T} = \frac{\sum_{i=1}^{T} C_i}{T} \tag{19}$$

where T is the continuous charging time, and C_i is the tariff at the moment i. In this section, $\bar{C}_{\Delta T}$ = 0.57 yuan/ kWh. The daily tariffs are shown in Table 2 [27].

Moreover, 9:00 to 11:00, 14:00 to 16:00 and 19:00 to 21:00 are the peak periods of electricity prices and peak periods of electricity consumption. After considering the comprehensive conditions, charging in the above time periods must be avoided to reduce the costs to users and the burden on the grid and maximize its benefits.

Table 2. Daily tariffs.

Time period	Electricity price	Time period	Electricity price
00:00–07:00	0.23 yuan/kWh	16:00–19:00	0.61 yuan/kWh
07:00–09:00	0.61 yuan/kWh	19:00–21:00	0.92 yuan/kWh
09:00–11:00	0.92 yuan/kWh	21:00–23:00	0.61 yuan/kWh
11:00–14:00	0.61 yuan/kWh	23:00–24:00	0.23 yuan/kWh
14:00–16:00	0.92 yuan/kWh		

The strategy proposed in this section can be divided into five modes based on parameter tuning: random charging queuing mode, tariff-guided queuing mode, stop-and-charge queuing mode, emergency charging mode and combined multi-objective queuing charging mode. Each mode has its own advantages and disadvantages. This strategy will focus on a new charging mode combining these four modes according to a certain ratio factor. The specific charging strategy is described in Table 3.

Table 3. Description of charging modes.

Mode	Model Description
Random charging queuing	When φ_4= 0, φ_1= 1, $SOC_{min} < SOC_{curr}$, $P = R > 0.5$, it indicates that charging is a random behavior that conforms to a uniform distribution. The vehicles are to be charged, and the charging priority of the vehicles is calculated and evaluated based on the current number of charging vehicles at the charging piles.
Tariff-guided queuing	When φ_4= 0, φ_1= 1, $SOC_{min} < SOC_{curr}$, $P = (1.5 - \bar{C}_{\Delta T}/\bar{C}_D) > 0.5$, it means that the current average cost is lower than the daily average cost–that is, the charging is started, and the user is encouraged to charge the EV with the lowest parking tariff. The charging priority is calculated, and the charging queue is entered for vehicles that need to be charged. If the charging piles are full, a waiting queue must be entered.
Stop-and-charge queuing	When $\varphi_4 = 0$, $\varphi_1 = 1$, $SOC_{min} < SOC_{curr}$, $P = (1.5 - T_{Charge}/T_{Parking}) > 0.5$, it indicates that if the parking time exceeds the charging time, the electric vehicle is charged immediately upon arrival (i.e., $T_{Charge} < T_{Parking}$). As the parking time decreases, the priority also decreases to ensure that the arrival moment priority P is at maximum.
Emergency charging	When φ_4= 1, it means that the emergency mode must be entered, and the EV must be charged immediately.

4. EV load estimation based on MC

In analyzing the correlation between EV driving behavior and EV charging behavior, some factors affecting the total charging power need to be extracted from the grid system. These characteristics include the number of EVs, charging pile information, EV battery characteristics and user behavior. The first three characteristics mentioned above can be assumed as known quantities, while the last user behavior characteristic cannot be predicted and can only be set as a variable and solved by the model. It is generally impossible to solve the above problems directly; hence, simulation is needed. In order to obtain a more suitable charging scheme, MC simulation is used to treat the EV charging problem as a nonlinear programming problem and to simulate multiple strategies. Various probability distributions are used to describe the driving behavior of EVs in daily life, which can improve the reliability of MC simulation. The number of EVs, charging pile information, EV battery characteristics and users' behavior are used as constraints to establish the objective function.

The data for the probability distribution fitting model used is based on [31], in which the analysis is limited to Monday through Friday. The probability density functions involved in the probability model include the BS distribution function, the gamma distribution function, the following location-scale distribution function and the normal distribution function. The distance per trip for EV users, the frequency of EV trips per day, the duration of each EV trip and the departure time of each EV trip are shown in Eq (1) to Eq (6), as described in Section 2. In order to obtain the performance indexes of different charging schemes, the EV charging data and EV trip data are first counted and then simulated using MC on the values. In the simulation process, outer limits are made for when the battery starts charging to enable the EV users to complete the travel plan, as shown in Eq (20) to Eq (21):

$$\Delta T_i = \frac{C_{Qi}}{W_Q} = \frac{1}{W_Q} * V * CAP * \left(1 - SOC_{begin,\ i}\right) \tag{20}$$

$$t_i \in (T_{i0}, T_{i1} - \Delta T_i) \tag{21}$$

where ΔT_i is the maximum continuous charging time, and C_{Qi} is the charging capacity of the EV. W_Q is the constant power, which comes from the grid and has a value of 15 kW. V indicates the voltage, and the value is 230 V. CAP is the battery capacity. The value of a large-capacity battery is 200 Ah, and the value of a small-capacity battery is 100 Ah. $SOC_{begin,\ i}$ denotes the initial state of the ith battery capacity, which is related to the distance traveled for each trip. t_i indicates the time when the EV starts charging, provided that the travel plan can be completed. T_{i0} indicates starting the period when the EV is idle, and T_{i1} indicates ending the period when the EV is idle.

An EV battery charge prediction model was developed to determine the daily battery charge and implemented using MC based on random sampling experiments. In h intervals, the total charging capacity in each interval is recorded as Eq (22), as follows:

$$R_j = \frac{1}{D} * \sum_{d=1}^{D} \left(\sum_{i=1}^{Q} r_{ji}(d) \right) \tag{22}$$

where R_j is the total charging capacity of the jth interval, D is the total number of days calculated, Q is the number of EVs in that time period, and $r_{ji}(d)$ is the charging capacity of the jth EV in the ith time period of the dth working day, as shown in Eq (23).

$$r_{ij}(d) = \frac{h_j}{60} * W_{pile}(d) * E_i \tag{23}$$

where h_j refers to the time the jth interval lasted, in minutes. $W_{pile}(d)$ is the power of the charging post in the *dth* working day. E_i is the charging efficiency of the *ith* EV, which depends on the material of the battery and the related technology, and is set to 0.9.

In this paper, the day is divided into 96 time periods of 15 minutes each (h = 15). Subdividing the day into 96 time periods can more accurately simulate the load on the grid, as the charging behavior of EVs affects the grid load. With this mechanism, the impact of the charging load of EVs on the grid can be better simulated [34]. It also helps to evaluate the charging behavior and driving behavior of EVs more realistically. In each 15-minute time period, the status of EVs, such as charging volume, remaining capacity and driving mileage, can be recorded more frequently, which helps to better collect and record data, more accurately model and represent the charging demand of EVs, and more accurately capture the changing trends and patterns of charging demand for charging strategy formulation. Additionally, it enables more accurate calculations of charging costs. Because electricity prices may vary during different time periods, the cost of charging EVs during different time periods can be calculated more accurately by subdividing the day into 96 time periods [35].

The convergence condition in the MC model is expressed as Eq (24). The entire MC simulation is repeated no less than 100 times.

$$\rho_j = \frac{\sqrt{VAR_{Load,\ j}(\bar{E})}}{\overline{E_J}} = \frac{\sigma_j(\bar{E})}{\overline{E_J}} \tag{24}$$

where ρ_j denotes the coefficient of variance of the system at the jth moment. $VAR_{Load,\ j}$ denotes the variance at the jth moment, $\overline{E_J}$ denotes the expected value at the jth moment, and σ_j denotes the standard deviation at the jth moment. The coefficient of variance ρ_j is set to be less than 0.5%.

4.1. *MC simulation process*

In order to complete the simulation for a day, the basic information has to be obtained first. The user's travel schedule and the number of miles traveled on that day are initialized, and the probability density function of the travel is calculated according to Eq (1) to Eq (6), which are determined by the user's travel pattern. The specific time period of charging for the user is determined according to the different charging strategies determined by the user, as well as the state of the EV trip and the battery characteristics. The state of the EV is divided into three: driving, charging and idle. After obtaining the EV status, we can calculate the specific charging time period and the specific travel time period of the EV under different strategies and obtain the full charging time of the EV sufficient to support the travel plan and the specific cost of the whole charging process.

The charging time period is calculated, as well as the number of EVs that need to be charged in the time period according to the simulation. Then, the users queue up according to the calculated charging priority of EVs; if there is no need to queue for that period, they can charge according to the original charging plan. If more vehicles are scheduled to charge in that period and need to wait in the queue, users must move back to the originally calculated charging time period until the charging time is available. After the queue charging is finished, the adequacy of the power of the trip can be judged by combining the specific travel time and the full charging time. If the power of the trip is sufficient, the plan will be successful. Otherwise, it will fail, and the trip will be canceled. The specific simulation process is shown in Figure 8.

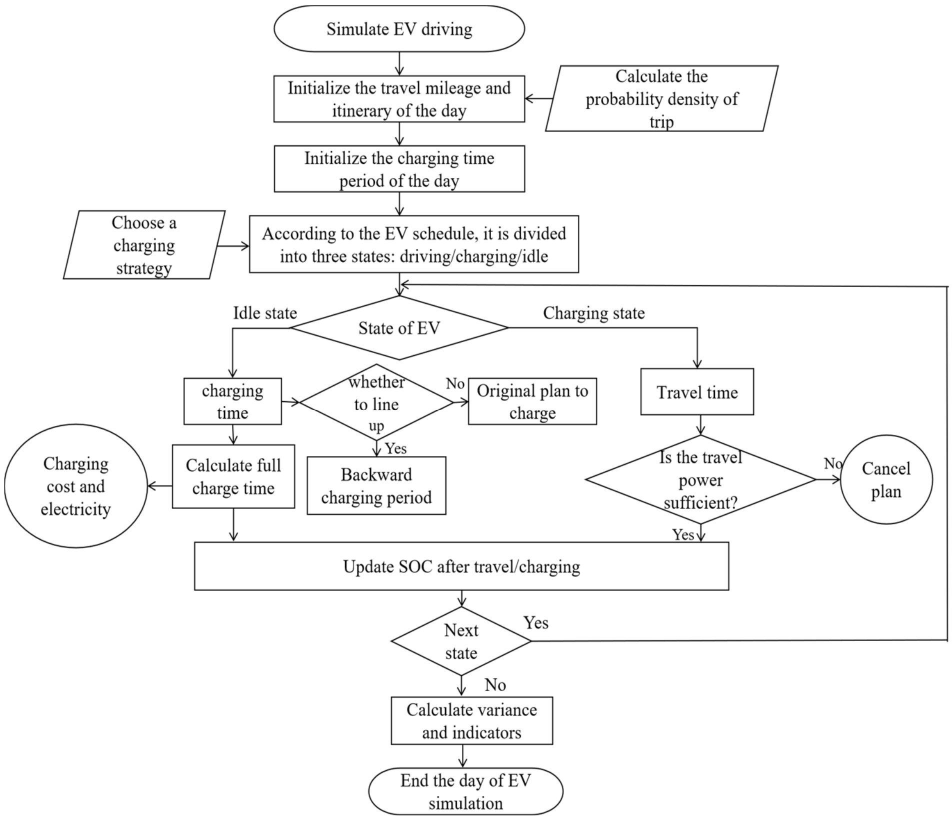

Figure 8. MC Simulation Process.

4.2. Queue operation

The pseudo-code of a complete queuing operation procedure:

```
Queuing Operation
Input: Probability density function Eq (1) to Eq (6)
(1) v_able_charge refers to the time period during which the vehicle can be charged.
(2) v_is_driving refers to the time period when the vehicle is in motion.
(3) total_evs refers to the total number of vehicles.
(4) total_periods refers to the total time period of the vehicle.
for ev=1 to total_evs
  [start, end]=Calculation_time_period (ev,v_able_charge,v_is_driving);
  The start time point and the end time point of the vehicle state change are calculated based on the time
  period when the vehicle is charged and the time period when the vehicle is being driven.
  v_is_charging=AdjustCharging(ev, start, end);
  The specific charging time period for each vehicle is determined based on the vehicle's travel and the
  four different strategies.
end for
for time=1 to total_periods
    charge_evs=v_is_charging (time);
    charge_evs represents the set of vehicles charged at the time period.
    if charge_evs≠ ∅
      for ev=1 to charge_evs
          Is_charging=ismember (ev,Charging_vehicles);
          Determine if the vehicle is already charging at the charging station.
          if Is_charging==true
            Continue;
          else
            P=Calculate_charging_priority (ev);
            P represents the set of priorities for each charging vehicle. It is calculated using Eq (9).

            [charge_star, charge_end]=cal_charge_time (ev);
            Calculate the start time period and end time period of charging for each vehicle.
          end if
      end for
          Charging_vehicles=Vehicle_charging (P,charge_star,charge_end);
          Vehicles with higher priority are added to the charging pile according to the charging priority
          order of the vehicles.
          Waiting_vehicles=Vehicle_waiting (P, charge_star, charge_end);
            Add vehicles that cannot be charged during the current time period to the queue for the queue.
    end if
end for
```

4.3. Selection of evaluation indexes and objective function

A comprehensive evaluation index system was designed based on several indicators that are currently of most interest to EV users (i.e., the success rate of the trip, the cost incurred when performing charging, the fluctuating peak load and the load variance), as shown in Eq (25) to Eq (28):

$$Y = \begin{cases} \|S_{trip}\| * \alpha + \|COST_{save}\| * \beta + \|APR\| * \gamma \\ \alpha + \beta + \gamma = 1 \end{cases} \quad (25)$$

$$S_{trip} = \frac{M_r}{M_p} \quad (26)$$

$$COST_{save} = \frac{Cost_r}{Cost_p} \quad (27)$$

$$APR = \frac{L_{mean}}{L_{max}} \quad (28)$$

where S_{trip} is the probability of the user's successful trip, $COST_{save}$ is the cost-saving rate caused by the scheme, APR is the average peak ratio, and α, β, γ are three positive weight coefficients whose values are less than or equal to 1. M_r indicates the actual mileage traveled, and M_p indicates the mileage planned for travel. $Cost_r$ indicates the actual cost of electricity, and $Cost_p$ indicates the maximum cost of electricity. L_{mean} denotes the average load, and L_{max} denotes the peak load. The values of α, β, γ can be flexibly adjusted according to the user's needs, where the parameter with the highest value represents the indicator that gives priority to the highest value (e.g., the highest value of α indicates that priority is given to the probability of successful trip for the user). For the evaluation index Y, the higher its value is, the better the performance of the system. $\alpha = 0.2, \beta = 0.5, \gamma = 0.3$ are taken in this study. The metrics are normalized with $\|\cdot\|$. The normalization process can better avoid premature algorithms and improve the sensitivity of the intelligent algorithm to the metrics. In this study, we set the integrated indicator L, as shown in Eq (29).

$$\|L\| = \left(\frac{l - L_{min}}{L_{max} - L_{min}}\right) \quad (29)$$

L_{max} denotes the upper bound of L, and L_{min} denotes the lower bound of L. For dividing 24 hours into 96 time periods, the resulting load variance VAR_{Load} during the period is defined as Eq (30) to Eq (32):

$$VAR_{Load} = \sqrt{\frac{1}{96}\sum_{j=1}^{96}\left(L_j - \bar{L}\right)^2} \quad (30)$$

$$L_j = L_{0j} + \sum_{i=1}^{n} L_{EVi} x_{ij} \quad (31)$$

$$\bar{L} = \frac{1}{96}\sum_{j=1}^{96} L_j \quad (32)$$

where $\bar{L}$ is the average value of the system load during a day, L_j is the sum of the base load and the charging load in time period j, and x_{ij} represents a variable of 0 or 1. When $x_{ij} = 1$, it means that the ith EV is charged in time slot j. On the contrary, when $x_{ij} = 0$, it means that the ith EV is not charged in time slot j. The objective function of the multi-objective queuing charging strategy is proposed and defined as Eq (33) to Eq (35):

$$M = \theta + S_5 + S_4[R\varphi_1 + (1.5 - \frac{\bar{C}_{\Delta T}}{\bar{C}_D})\varphi_2 + (1.5 - \frac{T_{Charge}}{T_{Parking}})\varphi_3 + F(s)] \tag{33}$$

$$s.t.\begin{cases} \sum_{i=1}^{3}\varphi_i = 1 \\ \theta \in [0,1] \\ SOC_{min} \end{cases} \tag{34}$$

$$Max\left\{F_{obj} = \left\{S_{trip}, COST_{save}, APR, M\right\}\right\} \tag{35}$$

In the above equation, φ_i are the coefficients in Eq (10) to Eq (12), S_4 and S_5 are shown in Eqs (13) and (14), and θ is the deviation of the model. F_{obj} is the objective function set, which considers the important parameters regarding the comprehensive evaluation index and optimizes the above parameters using the established nonlinear programming model. The values of the parameters (φ_i) are the parameters to be optimized. Some variables are still to be determined, and an intelligent optimization algorithm will be used to find the optimal solution in the model.

4.4. *Selection of intelligent algorithms*

In recent years, intelligent optimization algorithms have attracted much attention from researchers. Such artificial intelligence optimization algorithms can be used for various applications. The differential evolution (DE) algorithm has become one of the important algorithms in the field of optimization, given its power and simplicity [36]. Some classical algorithms, including simulated annealing (SA), genetic algorithm (GA), particle swarm optimization (PSO), whale optimization algorithm (WOA) [37], sparrow search algorithm (SSA) [38], and two-stage guided constraint differential evolution (TSGCDE), were selected to find the optimal value of the objective function. Due to the different algorithms, the final comprehensive evaluation index Y values differ due to the different parameters in the solved models. The number of iterations is set to 100, the dimension is set to 40D, and the population size is set to 100. $C_1 = 1.25$, $C_2 = 0.5$, and inertia weight $\omega = 0.9$ in the PSO. The selection ratio is 0.1, the crossover ratio is 0.7, and the variance ratio is 0.2 in the GA. Further, the annealing interval is 50 in the SA. The spiral shape parameter of the WOA algorithm is set to *b* = 1. The proportion of vigilantes *P* = 0.2 and the threshold of vigilance *ST* = 0.8 are set in the SSA algorithm. The TSGCDE algorithm has the dimension set to 40, the number of particles set to 100 and the boundary set to [–100,100]. The number of vehicles is set to 1000, and the number of charging piles is set to 300. The driving behavior of EVs is simulated for 30 days and 100 times. The final comprehensive evaluation index comparison of different algorithms is shown in Figure 9, and the specific charging load of 1000 vehicles is shown in Figure 10.

As shown above, the TSGCDE has the best overall maximum Y value of the solved comprehensive evaluation index compared with SA, GA, PSO, WOA and SSA. The Y value is also more stable, and the fluctuations are within a reasonable range. Overall, the load curve is the smoothest, the peak is the lowest, and the burden to the grid is the least. The comparison of the different algorithms' indexes for 1000 EVs is shown in Table 4.

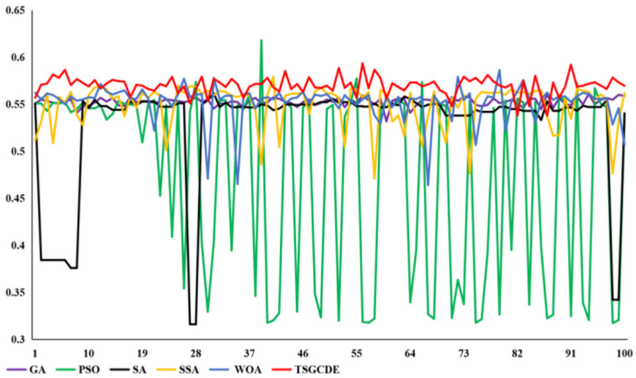

Figure 9. Comparison of comprehensive evaluation index Y of different algorithms.

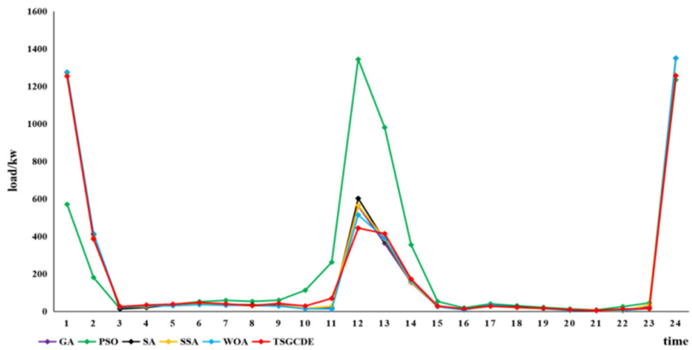

Figure 10. Comparison of load values of different algorithms.

Table 4. Comparison of different algorithmic indicators for 1000 EVs.

Parameter category	GA	PSO	SA	SSA	WOA	TSGCDE
Total load/ kW	4507.3	5593.9	4567.1	4546.5	4478.9	4422.5
Charging cost/ yuan	1564.0	2731.6	1599.0	1591.9	1542.3	1574.6
Cost savings rate	0.627	0.475	0.624	0.623	0.629	0.635
Average value/ kW	187.8	233.1	190.3	189.4	186.6	184.3
Peak value/ kW	1350.0	1344.5	1350.0	1350.0	1350.0	1257.2
Average peak ratio	0.139	0.173	0.141	0.140	0.138	0.147
Probability of successful travel	0.761	0.885	0.768	0.7703	0.774	0.836
Comprehensive evaluation index Y	0.553	0.471	0.527	0.546	0.557	0.570

According to the table, among the combined multi-objective queuing charging strategies, the TSGCDE produced the lowest total charging load of 4422.5 kW, the highest cost savings of 63.5%, the lowest peak value of 1257.2 kW and the highest overall index. Notably, the TSGCDE is used in the subsequent experiments.

5. Experimental analysis

The base load data of electricity consumption is adopted from [39]. The final total electricity consumption load can be obtained by superimposing the residential base load with the EV charging load. The specific residential base load is shown in Table 5.

The TSGCDE is selected for MC simulation, setting the dimension as 40, the number of particles as 100, the boundary as [−100,100], the vehicles as 1000, the number of charging piles as 300 and the vehicle-pile ratio as 3.3:1. 100 30-day simulations are conducted for EVs. The experimental results are all taken as the average of 100 simulations, and the specific charging load is shown in Figure 11. The total charging load curve can be obtained by superimposing the base and charging loads. The total charging load curve is shown in Figure 12.

Table 5. Base load of a day for residents of a neighborhood.

Time	Load/kW	Time	Load/kW	Time	Load/kW	Time	Load/kW
01:00	1670.4	07:00	1894.2	13:00	2230.7	19:00	2543.1
02:00	1740.4	08:00	2103.4	14:00	2263.8	20:00	2533.3
03:00	1699.8	09:00	2345.2	15:00	2242.4	21:00	2382.8
04:00	1605.1	10:00	2399.2	16:00	2243.4	22:00	2386.9
05:00	1776.6	11:00	2449.6	17:00	2382.8	23:00	1990.5
06:00	1830.4	12:00	2200.3	18:00	2402.3	24:00	1808.4

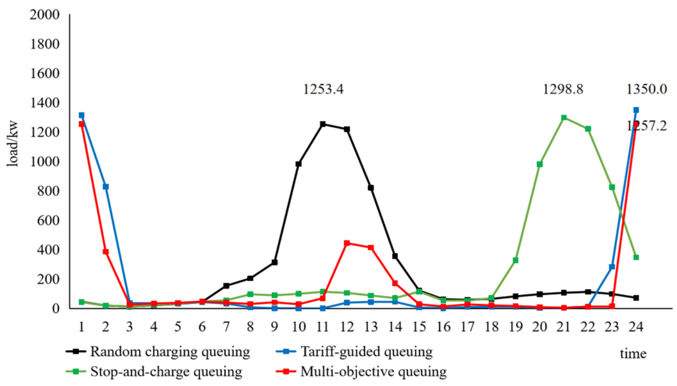

Figure 11. Charging load for 1000 vehicles under different strategies.

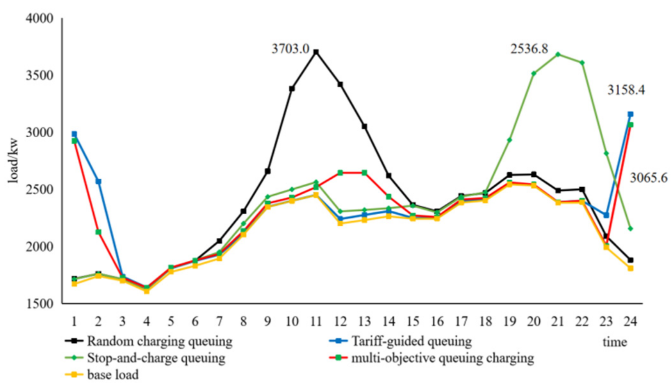

Figure 12. Base load with 1000 vehicles charging load superimposed under different strategies.

Figures 11 and 12 show that in the random charging queue mode, the peak charging period for EVs mainly occurs between 9:00 and 14:00, which highly coincides with the peak period of the residential base load, possibly causing pressure on the grid operation. Although the tariff-guided queuing charging model avoids the peak residential base load period, this model also has a major problem that causes a new charging peak period between 23:00 and 2:00, making the peak charging load as high as 3158.4 kW for a short period of time, which compromises the stability of the grid. Compared with the other three strategies, the charging load of EVs in the combined charging queuing strategy is relatively flat. Although a peak time period is also generated between 23:00 and 2:00, the charging load value is slightly lower compared with the tariff-guided queuing charging mode, which generally reduces the hazard to the grid. A comparison of specific indicators for different charging strategies for 1000 EVs is shown in Table 6.

The comparison results show that the total load generated by the tariff-guided queuing strategy is the lowest at 4217.6 kW. Further, the combined multi-objective queuing strategy is the second lowest, and the highest total load is the random charging queuing strategy. The tariff-guided queuing strategy is the lowest charging cost, which is only 1160.5 yuan, followed by the combined multi-objective queuing strategy and the highest random charging queuing strategy. For the overall cost-saving rate, the best is the tariff-guided queuing strategy, with a saving rate of 72.1%, followed by the combined multi-objective queuing strategy, with a saving rate of 63.5%. The lowest saving rate is the random charging queuing strategy. However, the tariff-guided queuing strategy produces the highest peak, the random queuing strategy produces the lowest peak, and the combined multi-objective queuing strategy produces a peak only slightly higher than the random queuing strategy. The specific charging costs for 1000 EVs under different strategies are shown in Figure 13, and the comprehensive evaluation index Y is shown in Figure 14.

Table 6. Comparison of indicators of different charging strategies for 1000 EVs.

Parameter category	Multi-objective queuing	Tariff-guided queuing	Stop-and-charge queuing	Random charging queuing
Total load/ kW	4422.5	4217.6	6254.2	6359.0
Charging cost/ yuan	1574.6	1160.5	4417.9	4539.4
Cost savings rate	0.635	0.721	0.236	0.216
Average value/ kW	184.3	175.7	260.6	265.0
Peak value/ kW	1257.2	1350.0	1298.8	1253.4
Average peak ratio	0.147	0.130	0.201	0.211
Probability of successful travel	0.836	0.668	0.940	0.939
Comprehensive evaluation index Y	0.570	0.537	0.405	0.397

The comparison results in the above figure show that the comprehensive evaluation index Y of the combined multi-target queuing strategy is still better than the other three charging strategies despite increasing the vehicle-pile ratio. However, compared to the vehicle-pile ratio of 3.3:1, the overall evaluation index Y decreases for all four charging strategies because the number of charging piles that can be used decreases by increasing the vehicle-pile ratio, and the waiting time for vehicles waiting in the queue for charging at the peak hour of charging is longer, largely affecting the travel plan and the charging cost. Consequently, the success rate of travel and the saving rate of charging costs are decreased.

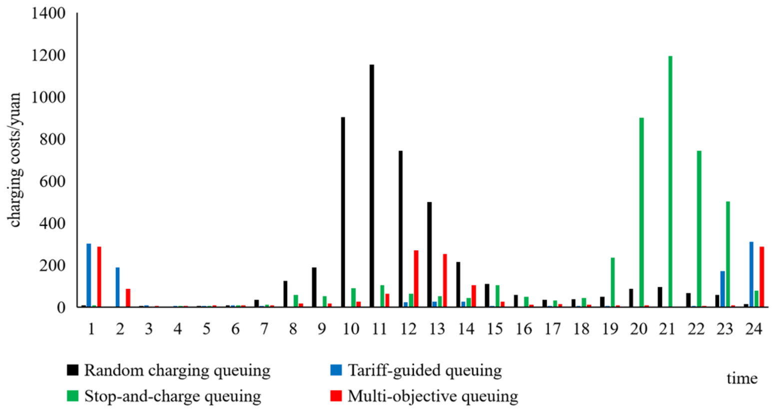

Figure 13. Specific charging costs for 1000 vehicles under different strategies.

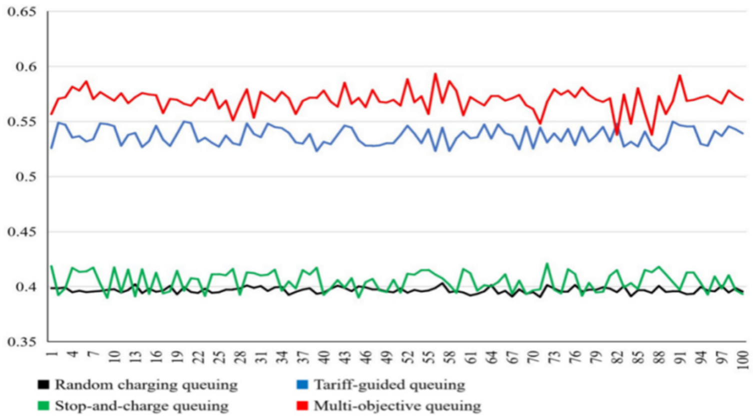

Figure 14. Comprehensive evaluation index of 1000 vehicles under different strategies.

The number of vehicles is set to 1000, and the number of charging piles is set to 155. The vehicle-pile ratio is 6.5:1. 100 30-day simulations are conducted for EVs, and the experimental results are all taken as the average of 100 simulations. The comprehensive evaluation index Y is shown in Figure 15.

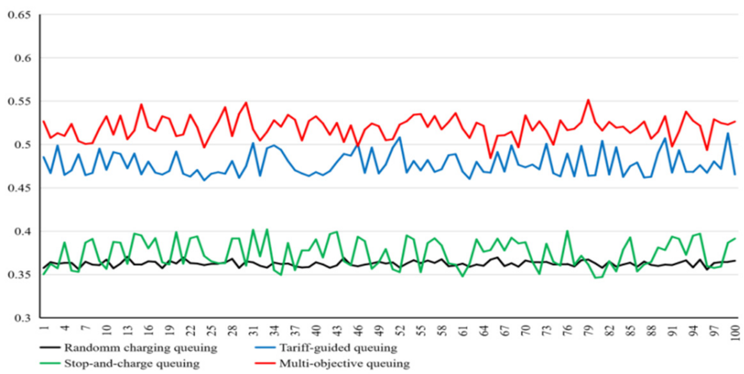

Figure 15. Increase the vehicle-pile ratio under 1,000 vehicles, comprehensive evaluation index.

The number of vehicles is set to 500, the number of charging posts is set to 167, and the vehicle-pile ratio is set to 3:1. The specific charging load is shown in Figure 16, and the total charging load is shown in Figure 17. It can be seen that the peak charging period of the four modes is similar in 1000 vehicles. The tariff-guided queuing charging mode still resulted in a new peak charging period from 23:00 to 2:00, with a high peak charging load of 2559.9 kW for a short time, which compromises the grid's stability. The comparison of specific indicators of different charging strategies for 500 EVs is shown in Table 7. Figure 18 shows the specific charging costs of 500 EVs under different strategies, and Figure 19 shows the evaluation index Y.

From the perspective of comprehensive evaluation indexes, the random charging queuing strategy still has the worst effect, and its index slightly decreases. Meanwhile, the indicator of the combined multi-objective queuing strategy remains the highest and shows the most desirable effect.

The number of vehicles is set to 500, the number of charging piles is set to 76, and the vehicle-pile ratio is set to 6.5:1. The comprehensive evaluation index Y is shown in Figure 20. The comprehensive evaluation index Y of the combined multi-objective queuing strategy is also better than the other three charging strategies.

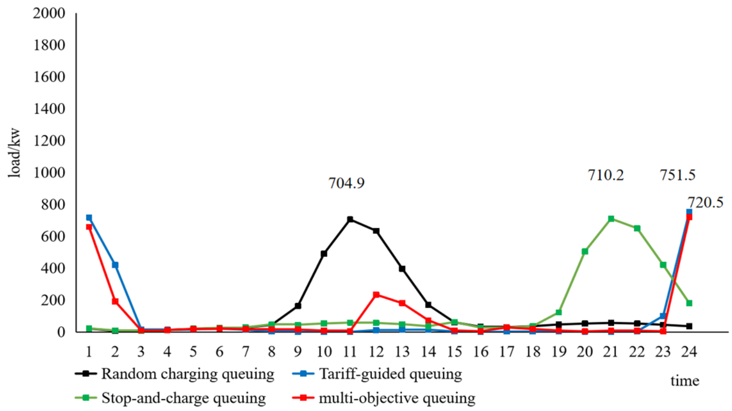

Figure 16. Specific charging load of 500 vehicles under different strategies.

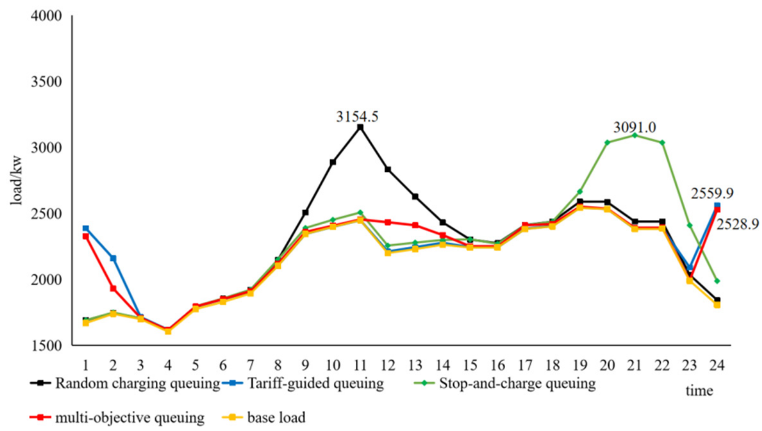

Figure 17. Base load with 500 vehicles charging load superimposed under different strategies.

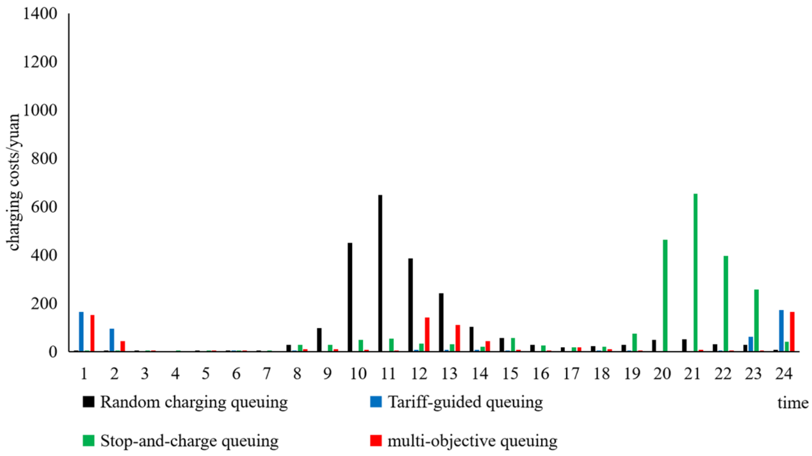

Figure 18. Specific charging costs for 500 vehicles under different strategies.

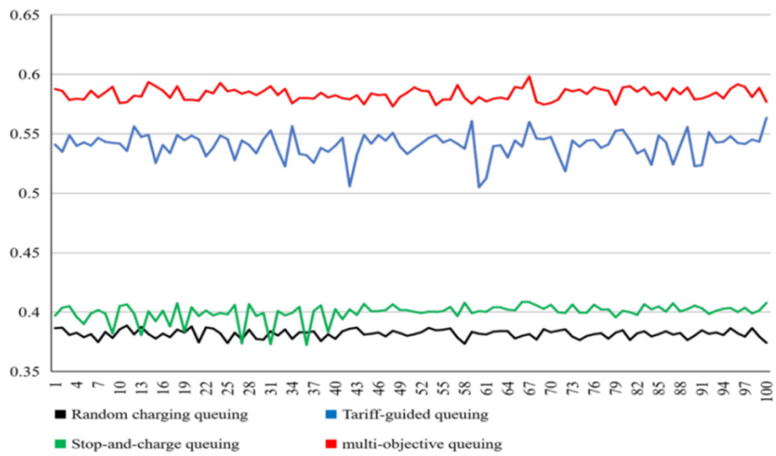

Figure 19. Comprehensive evaluation index of 500 vehicles under different strategies.

Table 7. Comparison of indicators of different charging strategies for 500 EVs.

Parameter category	Multi-objective queuing	Tariff-guided queuing	Stop-and-charge queuing	Random charging queuing
Total load/kW	2273.6	2130.1	3210.3	3164.6
Charging cost/yuan	772.8	553.0	2281.8	2306.4
Cost savings rate	0.635	0.721	0.236	0.216
Average value/kW	94.7	88.8	133.8	131.9
Peak value/kW	720.5	751.5	710.2	704.9
Average peak ratio	0.131	0.118	0.188	0.187
Probability of successful travel	0.851	0.702	0.954	0.947
Comprehensive evaluation index Y	0.583	0.540	0.400	0.382

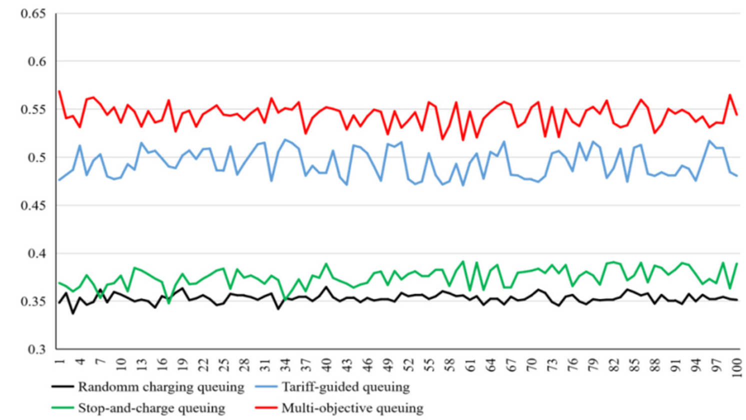

Figure 20. Increase the vehicle-pile ratio under 500 vehicles, comprehensive evaluation index.

Due to the limitation of the number of charging posts, the peak charging of the tariff-guided queuing mode and that of the combined multi-target queuing mode have a large degree of decrease compared to the original tariff-guided non-queuing mode and combined multi-target non-queuing mode in [24]. The load comparison is shown in Figure 21. The above figure shows that the original tariff-guided mode load peak is 8.61 times higher than the tariff-guided queuing mode load peak, and the original combined multi-objective mode load peak is 8.53 times higher than the combined multi-objective queuing mode load peak. Therefore, it is concluded that the queuing strategy reduces the load peak to a large extent and reduces the pressure on the grid, which is of greater significance.

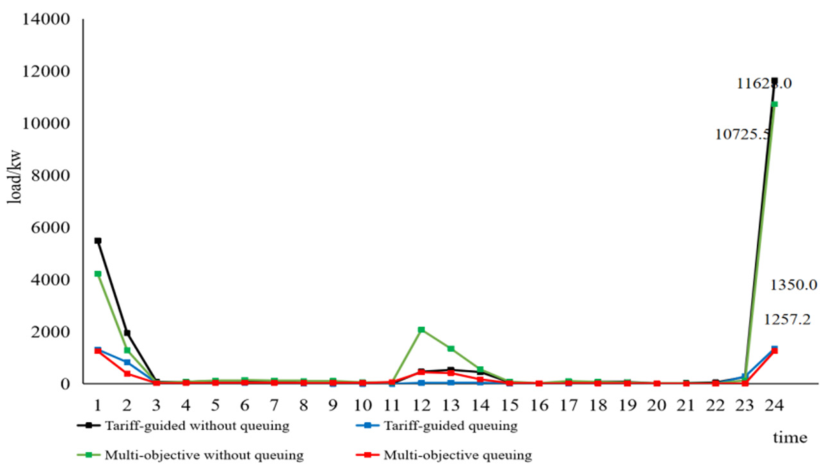

Figure 21. Comparison of 1000 vehicles queuing mode and original non-queuing mode.

In this study, the charging process of 100 EVs with combined multi-target queuing is demonstrated in detail. The charging piles are set to 15, and the peak charging time of combined multi-target queuing is selected for demonstration (i.e., the 93rd, 94th and 95th peak charging periods), as shown in Figures 22–24. When the remaining time is 0, the EVs on the charging pile will be finished charging at the beginning of the next time period, and the vehicles with the highest priority among the vehicles in the queue will enter the charging pile for charging in order. New vehicles waiting to be charged will be included in the charging queue.

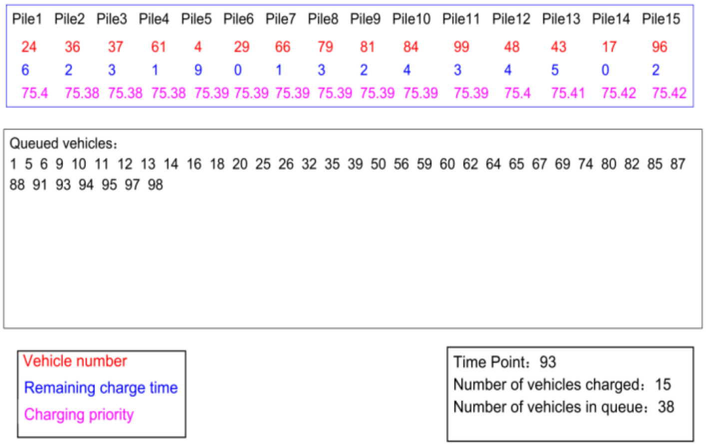

Figure 22. 93rd time period.

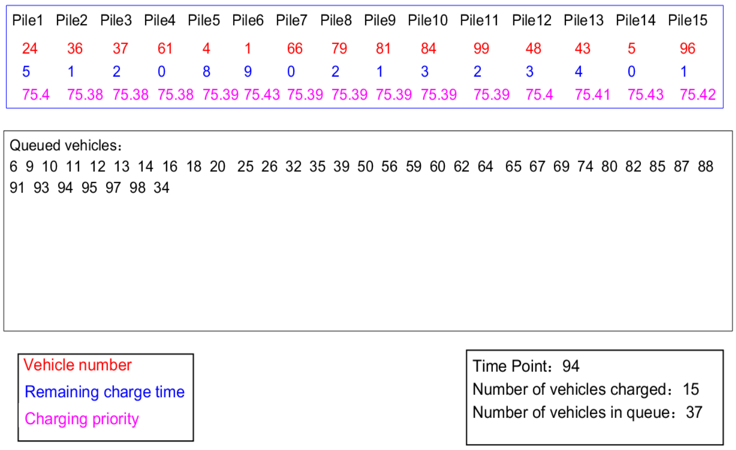

Figure 23. 94th time period.

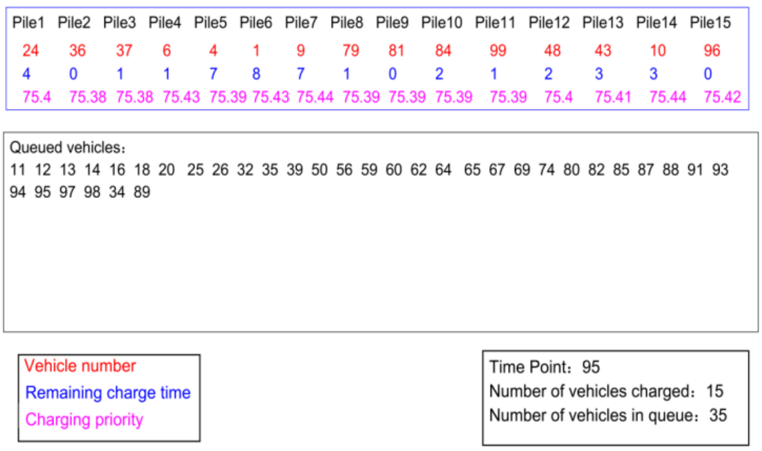

Figure 24. 95th time period.

6. Conclusions and future directions

This study explored EVs' driving and charging behaviors and proposes a multi-objective queuing charging strategy. By modeling the strategy, we combine common charging modes and consider the problem of the unbalanced vehicle-pile ratio that exists in these modes to introduce the problem of queuing charging of EVs. In particular, the problem of non-uniform battery capacity is considered, and the strategy is equipped with an emergency charging mode. The comparison results of multiple strategies show that the combined multi-objective queuing charging strategy has the highest comprehensive evaluation index and reduces the charging cost. The combined multi-target queuing charging strategy flattens the EV charging load curve and reduces the charging load peak. Compared with other modes, the combined multi-objective queuing mode largely reduces the burden of charging on the grid, achieves the highest comprehensive index, and realizes a win-win situation for both the supply and demand sides. The charging load of the tariff-guided queuing mode and the charging load of the combined multi-target queuing mode are also compared with the charging load without queuing. Further, the experimental results show for the charging peak of the tariff-guided queuing mode and the peak of the combined multi-objective queuing mode a large degree of reduction. Therefore, the proposed queuing strategy can largely reduce the pressure on the power supply side and improve grid stability.

Furthermore, this study focused on private EVs. It must be noted that there is a lack of research on electric buses and electric cabs. In subsequent research, more attention should be paid to the driving and charging laws of electric buses and electric cabs. Moreover, the base load data used in this paper is a residential community base load, which is not large. Thus, the charging load fluctuations caused by a small number of vehicles will have a greater impact on the overall load. Subsequent studies should choose a larger base load and expand the number of EVs.

Use of AI tools declaration

The authors declare they have not used artificial intelligence (AI) tools in the creation of this article.

Acknowledgments

This work was partially supported by the Fujian University of Technology under Grant GY-Z19005, GY-Z18183 and GY-Z20016.

Conflict of interest

The authors declare no conflict of interest.

References

1. H. S. Das, M. M. Rahman, S. Li, C. W. Tan, Electric vehicles standards, charging infrastructure, and impact on grid integration: A technological review, *Renewable Sustainable Energy Rev.*, **120** (2020), 109618. https://doi.org/10.1016/j.rser.2019.109618

2. S. Habib, M. Kamran, U. Rashid, Impact analysis of vehicle-to-grid technology and charging strategies of electric vehicles on distribution networks-A review, *J. Power Sources*, **277** (2015), 205–214. https://doi.org/10.1016/j.jpowsour.2014.12.020
3. Y. Zhou, X. Li, The state-of-art of the EV charging control strategies, in *2015 34th IEEE Chinese Control Conference (CCC),* (2015), 7916–7921. https://doi.org/10.1109/ChiCC.2015.7260898
4. G. Rajendran, C. A. Vaithilingam, N. Misron, K. Naidu, M. R. Ahmed, A comprehensive review on system architecture and international standards for electric vehicle charging stations, *J. Energy Storage*, **42** (2021), 103099. https://doi.org/10.1016/j.est.2021.103099
5. J. Zhang, J. Yan, Y. Liu, H. Zhang, G. Lv, Daily electric vehicle charging load profiles considering demographics of vehicle users, *Appl. Energy*, **274** (2020), 115063. https://doi.org/10.1016/j.apenergy.2020.115063
6. Y. Xiang, S. Hu, Y. Liu, X. Zhang, J. Liu, Electric vehicles in smart grid: a survey on charging load modelling, *IET Smart Grid*, **2** (2019), 25–33. https://doi.org/10.1049/iet-stg.2018.0053
7. H. B. Moon, S. Y. Park, C. Jeong, J. Lee, Forecasting electricity demand of electric vehicles by analyzing consumers' charging patterns, *Transp. Res. Part D: Transp. Environ.*, **62** (2018), 64–79. https://doi.org/10.1016/j.trd.2018.02.009
8. R. Tu, Y. Gai, B. Farooq, D. Posen, M. Hatzopoulou, Electric vehicle charging optimization to minimize marginal greenhouse gas emissions from power generation, *Appl. Energy*, **277** (2020), 115517. https://doi.org/10.1016/j.apenergy.2020.115517
9. O. Elma, A dynamic charging strategy with hybrid fast charging station for electric vehicles, *Energy*, **202** (2020), 117680. https://doi.org/10.1016/j.energy.2020.117680
10. Y. Kim, H. Kim, K. Suh, Environmental performance of electric vehicles on regional effective factors using system dynamics, *J. Cleaner Prod.*, **320** (2021), 128892. https://doi.org/10.1016/j.jclepro.2021.128892
11. A. Poullikkas, Sustainable options for electric vehicle technologies, *Renewable Sustainable Energy Rev.*, **41** (2015), 1277–1287. https://doi.org/10.1016/j.rser.2014.09.016
12. C. Chen, F. Shang, M. Salameh, M. Krishnamurthy, Challenges and advancements in fast charging solutions for EVs: A technological review, in *2018 IEEE Transportation Electrification Conference and Expo (ITEC)*, (2018), 695–701. https://doi.org/10.1109/ITEC.2018.8450139
13. M. Bilal, M. Rizwan, Electric vehicles in a smart grid: a comprehensive survey on optimal location of charging station, *IET Smart Grid*, **3** (2020), 267–279. https://doi.org/10.1049/iet-stg.2019.0220
14. G. Xu, B. Zhang, S. Zhang, Multi-energy Coordination and Schedule Considering large-scale electric vehicles penetration, in *2018 2nd IEEE Conference on Energy Internet and Energy System Integration (EI2)*, (2018), 1–5. https://doi.org/10.1109/EI2.2018.8582136
15. Z. Xiao, H. Li, T. Zhu, H. Li, Day-ahead optimal scheduling strategy of microgrid with EVs charging station, in *2019 IEEE 10th International Symposium on Power Electronics for Distributed Generation Systems (PEDG)*, (2019), 774–780. https://doi.org/10.1109/PEDG.2019.8807656
16. X. He, C. Tu, L. Wang, J. Li, Z. Li, Double-layer charging strategy for electric vehicles considering users' driving patterns, *Autom. Electr. Power Syst.*, **42** (2018), 64–69. http://doi.org/10.7500/AEPS20170731005
17. S. Sachan, N. Adnan, Stochastic charging of electric vehicles in smart power distribution grids, *Sustainable Cities. Soc.*, **40** (2018), 91–100. https://doi.org/10.1016/j.scs.2018.03.031

18. L. Yan, X. Chen, Y. Chen, J. Wen, A cooperative charging control strategy for electric vehicles based on multiagent deep reinforcement learning, *IEEE Trans. Ind. Inf.*, **18** (2022), 8765–8775. https://doi.org/10.1109/TII.2022.3152218
19. J. Ping, Z. Yan, S. Chen, A two-stage autonomous EV charging coordination method enabled by blockchain, *J. Mod. Power Syst. Clean Energy*, **9** (2020), 104–113. https://doi.org/10.35833/MPCE.2019.000139
20. S. Iqbal, A. Xin, M. U. Jan, S. Salman, A. U. M. Zaki, H. U. Rehman, et al., V2G strategy for primary frequency control of an industrial microgrid considering the charging station operator, *Electronics*, **9** (2020), 549. https://doi.org/10.3390/electronics9040549
21. J. S. Pan, B. Sun, S. C. Chu, M. Zhu, C. S. Shieh, A parallel compact gannet optimization algorithm for solving engineering optimization problems, *Mathematics*, **11** (2023), 439. https://doi.org/10.3390/math11020439
22. U. Akram, M. Khalid, S. Shafiq, A strategy for residential demand response management in modern electricity markets, in *2018 IEEE International Conference on Industrial Technology (ICIT)*, (2018), 1138–1142. https://doi.org/10.1109/ICIT.2018.8352338
23. W. Chen, L. Zheng, H. Li, X. Pei, An Assessment Method for the Impact of Electric Vehicle Participation in V2G on the Voltage Quality of the Distribution Network, *Energies*, **15** (2022), 4170. https://doi.org/10.3390/en15114170
24. M. Han, A V2G scheduling strategy based on the fruit fly optimization algorithm, *J. Phys.: Conf. Ser.*, **1952** (2021), 042063. https://doi.org/10.1088/1742-6596/1952/4/042063
25. T. W. Sung, P. W. Tsai, T. Gaber, C. Y. Lee, Artificial Intelligence of Things (AIoT) technologies and applications, *Wireless Commun. Mobile Comput.*, **2021** (2021), 9781271. https://doi.org/10.1155/2021/9781271
26. K. B. Lee, M. A. Ahmed, D. K. Kang, Y. C. Kim, Deep reinforcement learning based optimal route and charging station selection, *Energies*, **13** (2020), 6255. https://doi.org/10.3390/en13236255
27. Y. Zhou, Z. Li, X. Wu, The multiobjective based large-scale electric vehicle charging behaviours analysis, *Complexity*, **2018** (2018), 1968435. https://doi.org/10.1155/2018/1968435
28. V. C. Pedroso, C. A. Taconeli, S. R. Giolo, Estimation based on ranked set sampling for the two-parameter Birnbaum-Saunders distribution, *J. Stat. Comput. Simul.*, **91** (2021), 316–333. https://doi.org/10.1080/00949655.2020.1814287
29. A. Rahayu, P. Purhadi, S. Sutikno, D. D. Prastyo, Multivariate gamma regression: Parameter estimation, hypothesis testing, and its application, *Symmetry*, **12** (2020), 813. https://doi.org/10.3390/sym12050813
30. R. A. Verzijlbergh, Z. Lukszo, M. D. Ilić, Comparing different EV charging strategies in liberalized power system, in *2012 9th International Conference on the European Energy Market*, (2012), 1–8. https://doi.org/10.1109/EEM.2012.6254807
31. H. Wang, X. Zhang, L. Wu, C. Hou, H. Gong, Q. Zhang, et al., Beijing passenger car travel survey: implications for alternative fuel vehicle deployment, *Mitig. Adapt. Strateg. Glob. Change*, **20** (2015), 817–835. https://doi.org/10.1007/s11027-014-9609-9
32. T. Yi, C. Zhang, T. Lin, J. Liu, Research on the spatial-temporal distribution of electric vehicle charging load demand: A case study in China, *J. Cleaner Prod.,* **242** (2020), 118457. https://doi.org/10.1016/j.jclepro.2019.118457

33. S. Su, Method of location and capacity determination of intelligent charging pile based on recurrent neural network, *World Electr. Veh. J.*, **13** (2022), 186. https://doi.org/10.3390/wevj13100186
34. X. Yang, D. Niu, L. Sun, Z. Ji, J. Zhou, K. Wang, et al., A bi-level optimization model for electric vehicle charging strategy based on regional grid load following, *J. Cleaner Prod.*, **325** (2021), 129313. https://doi.org/10.1016/j.jclepro.2021.129313
35. F. Dandl, F. Fehn, K. Bogenberger, F. Busch, Pre-day scheduling of charging processes in mobility-on-demand systems considering electricity price and vehicle utilization forecasts, in *2020 Forum on Integrated and Sustainable Transportation Systems (FISTS)*, (2020), 127–134. https://doi.org/10.1109/FISTS46898.2020.9264862
36. T. W. Sung, B. Zhao, X. Zhang, An adaptive dimension differential evolution algorithm based on ranking scheme for global optimization, *PeerJ Comput. Sci.*, **8** (2022), 1007. https://doi.org/10.7717/peerj-cs.1007
37. S. Mirjalili, A. Lewis, The whale optimization algorithm, *Adv. Eng. Software*, **95** (2016), 51–67. https://doi.org/10.1016/j.advengsoft.2016.01.008
38. J. Xue, B. Shen, A novel swarm intelligence optimization approach: sparrow search algorithm, *Syst. Sci. Control Eng.*, **8** (2020), 22–34. https://doi.org/10.1080/21642583.2019.1708830
39. X. Yang, X. Bai, P. Li, H. Wei, Charging optimization of massive electric vehicles in distribution network, *Electr. Power Autom. Equip.*, **35** (2015), 31–36.